Original Article -Submission to AJRCCM

**TITLE**:

**Sequential $^{18}$F-fluorodeoxyglucose Positron Emission Tomography ($^{18}$F-FDG PET) scan findings in patients with extrapulmonary tuberculosis during the course of treatment - a prospective observational study**


**AUTHORS**:

**Jamshed Bomanji, Ph.D., Rajnish Sharma, MAMS, Bhagwant R Mittal, DNB, Sanjay Gambhir, DNB, Ahmad Qureshy, PhD, Shamim MF Begum, FANMB, Diana Paez, MD, Mike Sathekge, PhD, Mariza Vorster, PhD, Dragana Sobic Saranovic, PhD, Pawana Pusuwan, MD, Vera Mann, PhD, Sobhan Vinjamuri, PhD, Alimuddin Zumla, FRCP and Thomas NB Pascual, MD**

*All authors contributed equally

**INSTITUTIONAL AFFILIATIONS**:

**Jamshed Bomanji, MBBS, Ph.D.**: Institute of Nuclear Medicine, UCLH NHS Foundation Trust, 235 Euston Road, London NW1 2BU, UK. Email: jamshed.bomanji@nhs.net

**Rajnish Sharma, DRM, MAMS:** Director & Head , Division of Nuclear Medicine & PET Imaging, Specialist in Nuclear Medicine &Thyroid diseases, Molecular Imaging & Research Center ( MIRC), INMAS, Delhi. Email: drrsms@rediffmail.com

**Bhagwant Rai Mittal MD, DNB:** Professor & Head, Dept. of Nuclear Medicine & PET, Post Graduate Institute of Medical Education and Research, Sector 12, Chandigarh – 160012, India. Email: brmittal@yahoo.com

**Sanjay Gambhir, M.D., DNB:** Professor & Head, Dept. of Nuclear Medicine, SGPGIMS, Rae Bareli Road, Lucknow-226014 Email: gaambhir@yahoo.com

**Ahmad Qureshy, MBBS, PhD:** Institute of Nuclear Medicine and Oncology (INMOL) Hospital, New Campus Road, Lahore 54600, Pakistan. Email: aqureshy@yahoo.com

**Shamim Momtaz Ferdousi Begum**, DNM, FANMB: National Institute of Nuclear Medicine & Allied Sciences (NINMAS) 7th–10th Floor, Block-D, BSM Medical University Campus, Shahbag, Dhaka-1000, Bangladesh. Email: shamimmomtaz23@gmail.com

**Diana Paez, M.D.: Section Head,** Nuclear Medicine and Diagnostic Imaging Section, Division of Human Health, IAEA, Vienna, Austria. Email: D.Paez@iaea.org

**Mike Sathekge, M.D., Ph.D.:** Department of Nuclear Medicine, Steve Biko Academic Hospital, University of Pretoria, Pretoria, South Africa. Email: mike.sathekge@up.ac.za

**Mariza Vorster, M.D., Ph.D.:** Department of Nuclear Medicine, Steve Biko Academic Hospital, University of Pretoria, Pretoria, South Africa. Email: marizavorster@gmail.com

**Dragana Sobic Saranovic, M.D., Ph.D.:** Faculty of Medicine University of Belgrade and Center of Nuclear Medicine Clinical Center of Serbia, Belgrade, Serbia. Email: dsobic2@gmail.com

**Pawana Pusuwan, M.D.:** Division of Nuclear Medicine, Faculty of Medicine, Siriraj Hospital, Mahidol University, Bangkok-noi, Bangkok 10700, Thailand. Email: pawana.pus@mahidol.ac.th

**Vera Mann, Ph.D:** Institute of Nuclear Medicine, UCLH NHS Foundation Trust, 235 Euston Road, London NW1 2BU, United Kingdom. Email: verazmann@hotmail.com

**Sobhan Vinjamuri, MD, PhD:** Royal Liverpool University Hospital, Liverpool L7 8XP, United Kingdom Email: Sobhan.Vinjamuri@gmail.com

**Alimuddin Zumla, M.D., FRCP:** Center for Clinical Microbiology, Division of Infection and Immunity, University College London, and the National Institute of Health Research Biomedical Research Centre at UCL Hospitals, London, United Kingdom. Email: a.i.zumla@gmail.com

**Thomas NB Pascual, M.D.:** Section of Nuclear Medicine and Diagnostic Imaging, Division of Human Health, Department of Nuclear Sciences and Applications, International Atomic Energy Agency, Vienna International Centre, PO Box 100, 1400 Vienna, Austria. Email: T.Pascual@iaea.org

**Keywords:** Tuberculosis, Extrapulmonary tuberculosis, Imaging, $^{18}$F-FDG PET/CT scan, Monitoring Treatment, Biomarker, Disease activity, Relapse, Cure

**Word count:** **Main manuscript: 2769 words** **Abstract: 239 words**

**Displays:** **Figures: 7** **Tables: 5** **Supplemental Figure: 1**

**References:** **30**

**Corresponding Author:**

**Professor Jamshed Bomanji** FRCR, FRCP
Clinical Director, Institute of Nuclear Medicine,
5th Floor, UCLH NHS Foundation Trust,
235 Euston Road,
London NW1 2BU,
United Kingdom.
Email: jamshed.bomanji@nhs.net

**ABSTRACT**

**Background:**

Preliminary studies of Tuberculosis (TB) in macaques and humans using $^{18}$F-FDG Positron Emission Tomography (PET) imaging as a research tool suggest its usefulness in localising disease sites and as a clinical biomarker. Sequential serial scans in patients with extrapulmonary TB (EPTB) could provide information on the usefulness of PET-CT for monitoring response to therapy and defining cure.

**Patients and Methods:**

HIV-negative adults with EPTB from 8 sites across 6 countries had three $^{18}$F-FDG PET/CT scans: (i) within 2 weeks of enrolment, (ii) at 2 months into TB treatment and (iii) at end of ATT treatment. Scanning was performed according to the EANM guidelines. $^{18}$F-FDG PET/CT scans were performed 60±10 min after intravenous injection of 2.5–5.0 MBq/kg of $^{18}$F-FDG.

**Findings:**

147 patients with EPTB underwent three sequential scans. A progressive reduction over time of both the number of active sites and the uptake level (SUVmax) at these sites was seen. At the end of WHO recommended treatment: 53/147 (36.0%) patients had negative PET/CT scans, and 94/147 (63.9%) patients remained PET/CT positive, of which twelve patients had developed MDR TB. One died of brain tuberculoma.

**Interpretation:**

Current $^{18}$F-FDG PET/CT imaging technology cannot be used clinically as a biomarker of treatment response, cure or for decision-making on when to stop EPTB treatment. PET/CT remains a research tool for TB and further development of PET/CT is required using new *Mycobacterium tuberculosis*-specific tracers targeting high-density surface epitopes, gene targets, or metabolic pathways.



**Role of Funding Source and Oversight:** The International Atomic Energy Agency (IAEA) assisted in selection of recruitment centres with optimal $^{18}$F-FDG PET/CT imaging facilities and provided support for $^{18}$F-FDG PET/CT scans, consortium meetings and centralised facilities for data storage.

## INTRODUCTION

Tuberculosis (TB) remains the leading cause of death globally [1]. Upto 45% of the global burden of TB have extrapulmonary TB (EPTB) EPTB where patients receive TB therapy empirically based on clinical suspicion and utilising the current WHO management guidelines [7]. Furthermore, monitoring of treatment response in EPTB is based on either non-specific biochemical markers or clinical judgement. The decision to stop ATT after completion of the treatment course is usually based on recommendations from WHO guidelines and clinical judgement and is therefore subjective. This highlights a need for more accurate tools to define site(s) and extent of disease, evaluate response to therapy and detect relapse. Positron emission tomography (PET) using 2-deoxy-2-[fluorine-18] fluoro-D-glucose ($^{18}$F-FDG) provides functional information on sites of active inflammation and, in combination with CT data, delivers functional and anatomical information in a single scan [8, 9]. Preliminary studies on TB in macaques [10-13] and humans [14-19] employing $^{18}$F-FDG PET/CT as a research tool have suggested that it might be of clinical value for localisation of disease sites and assessment of treatment response. Currently there are several ongoing research studies on the application of PET/CT as a biomarker of treatment response in new drug combination trials and for insight into pathogenesis. Studies of EPTB patients under programmatic conditions with sequential serial scans may provide further information on the usefulness of PET-CT in monitoring response to therapy and defining cure. We recently published a study of the use of $^{18}$F-FDG PET/CT imaging to assess the extent of disease and common sites involved at first presentation in 358 patients with EPTB [20] . Here we present imaging findings from 147 $^{18}$F-FDG PET/CT patients with EPTB for whom three sequential $^{18}$F-FDG PET/CT scans were obtained during the entire course of WHO-recommended EPTB treatment.

## METHODS:

### Patients with EPTB and PET/CT scans

147 HIV-negative patients with EPTB from eight centres, located in six countries, who completed three sequential $^{18}$F-FDG PET/CT scans during the entire course of WHO-recommended EPTB treatment were studied. Patients were adults $\geq$18 years who fulfilled WHO criteria for EPTB, with either: positive culture for drug sensitive *M. tuberculosis* in any clinical specimen, positive nucleic acid amplification (GeneXpert MTB Rif/Assay; Cepheid, Sunnyvale, CA, USA), or presence of caseating granulomas with detection of acid-fast bacilli in a clinical biopsy or aspirate specimen.

### Anti-TB Treatment (ATT)

Patients received WHO-recommended ATT EPTB regimens [21]: 6 months usually, and in patients with bone and CNS involvement treatment was continued for 9–12 months.

**Frequency and Timing of $^{18}$F-FDG PET/CT Scans:**

Patients underwent three $^{18}$F-FDG PET/CT scans (non-contrast CT): (i) within 2 weeks of enrolment, (ii) at 2 months into ATT treatment and (iii) at the end of ATT treatment (**Table 1**).

**$^{18}$F-fluorodeoxyglucose (FDG) Positron Emission Tomography/Computerised Tomography (PET/CT):**

Scanning was performed according to the EANM guidelines.[9] $^{18}$F-FDG PET/CT scans were performed 60±10 min after intravenous injection of 2.5–5.0 MBq/kg of $^{18}$F-FDG. All $^{18}$F-FDG PET/CT scans were performed on the same scanner as was used for the baseline study. $^{18}$F-FDG is known to accumulate at sites of infection and inflammation. The inflammatory cells produce an excess of glycolytic enzymes and also over-express glucose transporter (GLUT) isotypes (mainly GLUT-1 and GLUT-3). The $^{18}$F-FDG PET component of the PET/CT provides the metabolic measure of activity as $SUV_{max}$ values.[22] The CT component of PET/CT provides the measure of radio-opacity, or density, of anatomical structures, expressed in Hounsfield units (HU). CT measurements of size (mm) are less prone to variability than $^{18}$F-FDG PET measurements of metabolic activity expressed as $SUV_{max}$ values.

**Patient Follow-up:**

Patients were followed up monthly for the first 2 months, and every 2 months thereafter until end of treatment completion. Drug resistance TB was confirmed using molecular Xpert MTB/RIF assay or culture based. Community acquired bacterial pneumonia was confirmed based on the demonstration of a new airspace infiltrate on a chest radiograph or CT in the presence of recently acquired respiratory signs and symptoms (cough and fever lasting 2–3 days).

**Data Collection and Analyses:**

Standardised clinical forms were used for entering patient biodata, demographic, clinical and laboratory data, including age, gender, HIV status, clinical signs and symptoms, physical findings, suspected clinical site of EPTB and $^{18}$F-FDG PET/CT findings. Central review of images and collection of data forms was established according to IAEA regulations. Clinical, radiological (dicom format) and microbiologic information were coded and sent to a central repository at the IAEA in Vienna and the core study centre in London for analysis. All data were transferred to the central coordinating site at University College Hospital, United Kingdom for analyses.

**Statistical Analysis:**

Descriptive statistics were used to summarise patients' characteristics; for continuous variables, median and interquartile ranges were given. For categorical variables, proportions falling into different categories were calculated. Multilevel mixed-effects linear regression models, to account for the multi-centre nature of the study and for serial PET scans on the same patients, were explored to investigate the change in $^{18}$F-FDG PET/CT findings over time. For this purpose, the sum of the $SUV_{max}$ values across all positive sites was calculated for each patient at each visit, by adding together $SUV_{max}$ values at all body sites where the $SUV_{max}$ values were at least 2.5 or more. The percentage decrease or increase in $SUV_{max}$ was calculated at median time intervals of the second and third visits (Appendix- **supplemental Figure 1**).

Statistical analysis was performed using Stata version 15 (SE 15 data version, StataCorp, 2017. *Stata Statistical Software: Release 15*. College Station, TX: StataCorp LLC).

**Interpretation of $^{18}$F-FDG PET/CT Scans:**

Scans were reported as positive or negative. A positive scan was defined as abnormally increased $^{18}$F-FDG uptake in a lesion (with CT correlate) which is greater than surrounding background and not explained by normal physiological organ uptake. The increase in metabolic activity was quantified by measuring the standardised uptake values ($SUV_{max}$). Maximum standardised uptake values ($SUV_{max}$) are a relative measure of FDG metabolism. Increase in metabolic activity was quantified by measuring the standardised uptake values ($SUV_{max}$).

## RESULTS:

**Study Population:**

147 patients with EPTB (77 females, age range: 18-82 years, median 28 years, IQR [21, 38 years]; and 70 males, age range 18-77 years, median 31.5 years, IQR [24, 50]) completed three sequential PET/CT scans. Of the 147 patients, 76 gave a history of weight loss at baseline presentation (51.7%), 26 patients at second visit (17.7%) and 22 patients at third visit (15.0%). Night sweats were documented in 48 patients at presentation (32.6%), 16 patients at second visit (10.9%) and 11 patients at third visit (7.5%). Of the 147 patients, 75 gave a history of fever at baseline presentation (51%), 31 patients at second visit (21.1%) and 17 patients at third visit (11.6%).

### Time to scan and number of active sites

**Table 2** shows time to scan and number of active sites in 147 patients with EPTB who underwent all three 18F-FDG PET/CT scans. In most patients both the number of active sites and the uptake level ($SUV_{max}$) at these sites showed a progressive reduction over time during treatment duration (**Figures 1, 2, 3)**

**Baseline scan and anatomical location of active sites**

**Table 3** shows the anatomical location of $^{18}$F-FDG PET/CT positive EPTB sites of 147 patients and $SUV_{max}$ values in the positive anatomical sites.

**Sequential $^{18}$F-FDG PET/CT Scans over Time**

**Tables 4 and 5,** show the number of active disease sites in all 147 patients with EPTB over the treatment period. 53 of 147 patients (36.0%; 29 females, 24 males) became PET negative at the end of treatment (examples of scans are given in **Figures 1, 2, 3).** However, 94/147 patients (63.9%) showed a positive third scan (**Figure 4**). Of these, one patient developed a brain tuberculoma and died (**Figure 5),** and 12 patients were found to have MDR TB (example **Figure 6)** and were placed on appropriate MDR TB treatment

**Change in the Sum of PET/CT $SUV_{max}$ Values over Time**

The average sum of $SUV_{max}$ at all abnormal sites on baseline $^{18}$F-FDG PET/CT was 19.4 (95% CI 16.2–22.6) with a random variance of 14.1 between centres. Progressive reduction in activity was seen in most patients after 2 months of treatment. The reduction in the sum of $SUV_{max}$ averaged to 1.4/month (slope = -1.4, 95% CI -1.8/month – -1.1/month) with variance of the random slope at the centre level of 0.11 (95% CI 0.02–0.63; LR test for random slope: $\chi^2$=4.42, p=0.036). There was no significant difference in the slope by patients within centres (the random effect of the slope on patient level was not significant; LR test for random slope: $\chi^2$=0, p=1). The predicted sum of $SUV_{max}$ at the median time of the second $^{18}$F-FDG PET/CT scan (2.5 months) was 15.8 (equivalent to a fall of 18.6% in the sum of $SUV_{max}$). At the median time of the third scan (7.4 months), the predicted sum of $SUV_{max}$ was 8.8 (equivalent to a fall of 54.6% in the sum of $SUV_{max}$).

In two patients there was a five-unit rise in $SUV_{max}$ values at the second visit, attributed to superadded community-acquired pneumonia (**Figure 7**); in both patients the $SUV_{max}$ values had declined at the third visit. In 12 patients, $SUV_{max}$ values showed a reduction at the second visit but increased significantly at the third scan; these patients were found to have MDR TB.

**Management outcomes at 6 months post-treatment follow-up**

At 6 months post-treatment follow-up, four patients had died, 123 were alive and well, and 14 had been lost to follow-up.

## DISCUSSION

There are several notable findings from our study. *First*, two-thirds of EPTB cases continued to show active disease sites after the end of WHO-recommended treatment for EPTB, indicating that it cannot be used as a biomarker of treatment response. *Second*, this raises questions regarding the duration of therapy and the definitions of 'cure', 'persistence of disease', and 'relapse'. *Third*, increased or persistent $^{18}$F-FDG PET activity occurred in patients who developed secondary infection. *Fourth*, persistent $^{18}$F-FDG PET activity led to further investigation resulting in a diagnosis of development of MDR TB in 12 patients who required change to appropriate treatment. *Fifth*, $^{18}$F-FDG PET/CT scan cannot distinguish non-specific inflammation from that specific to replicating mycobacteria or residual inflammatory activity after treatment.

Our study shows that whilst there was a progressive overall fall in metabolic activity ($^{18}$F-FDG activity) in response to treatment, the decreasing trend was not present in all EPTB patients. Increased or persistent activity at follow-up indicated superadded infection or development of MDR TB. $^{18}$F-FDG PET/CT remained positive in 63.9% of patients after completion of WHO-recommended ATT regimens, suggesting that the chronic inflammatory response in EPTB may continue for some time. There are currently no established criteria for defining the end of treatment apart from clinical symptoms and biochemical biomarkers, which were not raised in more than 50% of our patients. It may be that individual tissue and organ types respond to treatment at different rates due to variable immune responses. In animal studies, lymph nodes have been found to have different PET activity trajectories even within the same animal [23]. Studies of spinal TB have shown that 50% of patients have magnetic resonance imaging evidence of activity even after 12 months of treatment [18,24]. In bone and joint TB, radiological markers have been used to assess cure. However, plain X-rays may never return to baseline. Studies on TB lymphadenitis have shown that continued presence of nodes at end of treatment does not always signify an unfavourable outcome and our own data show residual node activity may be present after treatment. Thus $^{18}$F-FDG PET/CT cannot be used to decide when to stop EPTB treatment.

The exclusion of HIV-positive patients was designed to preclude any influence of confounding co-morbidities and co-infections. It should be noted, however, that detection of extrapulmonary lesions may be particularly useful in such patients since they could be due to a variety of infectious or non-infectious complications of HIV/AIDS. The role of $^{18}$F-FDG PET/CT in HIV-infected patients was recently addressed in a small study of 18 HIV/TB patients [15]. After 2 months of treatment, 78% of patients had a significant metabolic response. Lymph node metabolic response was heterogeneous, with 57% of LN sites showing decreased $SUV_{max}$ and 41%, unchanged $^{18}$F-FDG uptake. $^{18}$F-FDG PET/CT showed a complete metabolic response after TB treatment in only 47% of patients.

In mouse, rabbit and primate models, $^{18}$F-FDG PET/CT has been used to display progression of disease after exposure to *M. tuberculosis* and the response to treatment [1–4]. Previous human studies using $^{18}$F-FDG PET/CT scanning to monitor ATT response have shown that there is decreased metabolic activity after 1 month treatment of pulmonary (n=10) and extra-pulmonary (n=10) TB [5], a steady decline in uptake after 6, 12 and 18 months of treatment of skeletal TB (n=18) [6] and no significant uptake in PTB (n=8) after a year of treatment [7]. PET and CT have shown complementary results in the detection and response monitoring of pulmonary and extra-pulmonary TB [8]. It has also been shown that there can be enhanced cellular activity without a change in nodal size as measured on CT.

In animal TB model studies an increase in $^{18}$F-FDG activity, reflected by $SUV_{max}$ values, was proportional to the number of *M. tuberculosis* bacilli in caseating granulomas [25]. Recent work in non-human primates suggests that the TB disease state may be more dynamic than previously believed and that *M. tuberculosis* infection may induce a diverse spectrum of disease, where after treatment the immune response keeps infection of slow-replicating mycobacteria at the subclinical level. *M. tuberculosis* mRNA was detected in non-resolving and intensifying lesions on PET/CT images, suggesting that even apparently curative treatment for PTB may not eradicate all *M. tuberculosis* bacteria [26]. Continuing activity may also represent continuing immune responses against slow-responder mycobacterial populations, which differ in their intrinsic drug susceptibility [27]. Thus long-term follow-up is required to monitor for relapse. An ongoing large prospective, multi-centre randomised, phase 2b, non-inferiority clinical trial (Predict TB Trial) of pulmonary TB participants is designed to shed more light on the usefulness of PET/CT as a biomarker for early prediction of treatment response [28]. PET/CT scans are being done at weeks 0, 4 and 16 or 24 and the authors hypothesise that PET/CT characteristics at baseline, PET/CT changes at 1 month and markers of residual bacterial load will identify individual patients with TB who can be cured with 4 months (16 weeks) of standard treatment and that PET/CT provides an opportunity to study other immunological or transcriptional signatures.

The current challenge for TB-specific PET/CT is the development of new *M. tuberculosis*-specific tracers targeting high-density surface epitopes, gene targets or metabolic pathways. A recent study developed a multi-drug treatment model in rabbits with experimentally induced TB meningitis and performed serial non-invasive dynamic $^{11}$C-rifampin PET over 6 weeks, demonstrating that rifampicin penetration into infected brain lesions is limited and spatially heterogeneous and decreases rapidly as early as 2 weeks into treatment [29]. These data demonstrate the proof of concept of PET as a clinically translatable tool for non-invasive measurement of intralesional antimicrobial distribution in infected tissues that might be useful in establishing individualised treatment regimens.

Our study is subject to several limitations. $^{18}$F-FDG PET/CT scans are designed to detect glucose metabolism and are therefore not specific for detection of TB lesions and cannot differentiate between infection and tumours [30]. Relatively high tracer uptake in normal brain grey matter hinders detection of brain tuberculomas and meningeal involvement. Moreover, small lesions ($\leq$1 cm) are very likely to be missed owing to partial volume effects. $^{18}$F-FDG PET/CT also has low sensitivity for the detection of small EPTB lesions in the kidney and urinary bladder, which are masked by high tracer uptake due to the contribution of these organs to physiological $^{18}$F-FDG tracer excretion.

**CONCLUSIONS:**

Whilst earlier studies showed $^{18}$F-FDG PET/CT showed promise as a non-invasive imaging technique for detection of the extent of EPTB disease, and as a biomarker of treatment response and cure, $^{18}$F-FDG PET/CT in its current form will remain mainly a research tool. The presence of active lesions after completion of WHO-recommended EPTB treatment regimens in a large number of cases requires further study. The potential of $^{18}$F-FDG PET/CT in further elucidating the spectrum of disease, the pathogenesis of EPTB and the effects of treatment on active lesions over time, including in HIV-infected, paediatric and MDR TB patients, requires longitudinal cohort studies of those with microbiologically confirmed and clinically suspected cases, twinned with biopsy and molecular studies over longer periods. Although use of $^{18}$F-FDG PET/CT for the clinical management of EPTB has conceptual appeal for identification of site of lesion for biopsy purposes, further development of the technique is required before a specific role can be determined for its use as a biomarker of disease activity, defining cure or relapse.

**AUTHOR ROLES:** Jamshed Bomanji, Thomas NB Pascual and Alimuddin Zumla developed the concept and initiated discussions which led to the formation of the consortium. Rajnish Sharma, Bhagwant Rai Mittal, Sanjay Gambhir, Ahmad Qureshy, Shamim Momtaz Ferdousi Begum, Mike Sathekge, Mariza Vorster, Dragana Sobic Saranovic and Pawana Pusuwan led the study sites. Sobhan Vinjamuri conducted quality assessment of imaging data. Olga Morozova collated the CRFs. Vera Mann performed the data analyses. Jamshed Bomanji led the imaging studies and, with Alimuddin Zumla, Diana Paez and Thomas NB Pascual, developed the first and final drafts of the manuscript. All authors contributed to data interpretation and writing of the manuscript.

**CONFLICTS OF INTEREST:** All authors declare no conflicts of interest.

**ACKNOWLEDGEMENTS:** AZ and JB acknowledge support from the NIHR Biomedical Centre at UCL Hospitals Foundation NHS Trust. AZ holds an NIHR senior Investigator award, and he is member of the Pan-African Network on Emerging and Re-emerging Infections and thank the European and Developing Countries Clinical Trials Partnership, EU Horizon 2020.

**REFERENCES**:


1 WHO (2019). Global Tuberculosis Report 2019. https://www.who.int/tb/publications/global_report/en/ Accessed 10th December 2019

2 Sharma SK, Mohan A. Extrapulmonary tuberculosis. Indian J Med Res, **2004**; 120: 316–353.

3 Sreeramareddy CT, Panduru KV, Verma SC, Joshi HS, Bates MN. Comparison of pulmonary and extrapulmonary tuberculosis in Nepal-a hospital-based retrospective study. BMC Infect Dis, **2008**; 8: 8.

4 Ilgazli A, Boyaci H, Basyigit I, Yildiz F. Extra pulmonary tuberculosis: Clinical and epidemiologic spectrum of 636 cases. Arch Med Res, **2004**; 35: 435–341.

5 Solovic I, Jonsson J, Korzeniewska-Koseła M, et al. Challenges in diagnosing extrapulmonary tuberculosis in the European Union, 2011. Euro Surveill, **2013**; 18(12). pii: 20432.

6 Kulchavenya E. Extrapulmonary tuberculosis: are statistical reports accurate? Ther Adv Infect Dis **2014**; 2: 61–70.

7 World Health Organization. Improving the diagnosis and treatment of smear-negative pulmonary and extrapulmonary tuberculosis among adults and adolescents. **2006**. https://www.who.int/tb/publications/2006/tbhiv_recommendations.pdf. Accessed 4 October 2018.

8 Zhuang H, Alavi A. 18-Fluorodeoxyglucose positron emission tomographic imaging in the detection and monitoring of infection and inflammation. Semin Nucl Med, **2002**; 32: 47–59.

9 Boellaard R, Delgado-Bolton R, Oyen WJ, et al. FDG PET/CT: EANM procedure guidelines for tumour imaging: version 2.0. Eur J Nucl Med Mol Imaging **2015**; 42: 328–354.

10 Coleman MT, Maiello P, Tomko J, et al. Early changes by (18)fluorodeoxyglucose positron emission tomography co-registered with computed tomography predict outcome after Mycobacterium tuberculosis infection in cynomolgus macaques. Infect Immun, **2014**; 82: 2400–2404.

11. Lin PL, Coleman T, Carney JP, et al. Radiologic responses in cynomolgous macaques for assessing tuberculosis chemotherapy regimens. Antimicrob Agents Chemother, 2013; **57:** 4237–4244.

12. Coleman M, Chen R, Lee M. PET/CT imaging reveals a therapeutic response to oxazolidinones in macaques and humans with tuberculosis. Sci Transl Med, 2014; **6:** 1–10.

13. Via LE, Schimel D, Weiner DM, et al. Infection dynamics and response to chemotherapy in a rabbit model of tuberculosis using [$^{18}$F]2-fluoro-deoxy-D-glucose positron emission tomography and computed tomography. Antimicrob Agents Chemother, 2012; **56:** 4391–4402.

14 Martinez V, Castilla-Lievre MA, Guillet-Caruba C, et al. (18)F-FDG PET/CT in tuberculosis: an early non-invasive marker of therapeutic response. Int J Tuberc Lung Dis, **2012**; 16: 1180–1185.

15 Martin C, Castaigne C, Vierasu I, Garcia C, Wyndham-Thomas C, de Wit S. Prospective serial FDG PET/CT during treatment of extrapulmonary tuberculosis in HIV-infected patients: an exploratory study. Clin Nucl Med, **2018**; 43: 635–640.

16 Dureja S, Sen I, Acharya S. Potential role of F18 FDG PET/CT as an imaging biomarker for the

non-invasive evaluation in uncomplicated skeletal tuberculosis: a prospective clinical observational. Eur Spine J, **2014**; 23: 2449–2454.

17 Stelzmueller I, Huber H, Wunn R, et al. 18F-FDG PET/CT in the initial assessment and for follow-up in patients with tuberculosis. Clin Nucl Med, **2016**; 41: e187–194.

18 Jain A, Goyal MK, Mittal BR, et al. 18FDG-PET is sensitive tool for detection of extracranial tuberculous foci in central nervous system tuberculosis - Preliminary observations from a tertiary care center in northern India [published online ahead of print, 2019 Nov 27]. J Neurol Sci. 2019;409:116585. doi:10.1016/j.jns.2019.116585

19 Jeon I, Kong E, Kim SW. Simultaneous 18F-FDG PET/MRI in tuberculous spondylitis: an independent method for assessing therapeutic response - case series. BMC Infect Dis. 2019;19(1):845. Published 2019 Oct 15. doi:10.1186/s12879-019-4469-2

20. Bomanji J, Sharma R, Mittal BR, et al. Eur Respir J. 2019 Dec 12. pii: 1901959. doi: 10.1183/13993003.01959-2019. [Epub ahead of print]

21. Gilpin C, Korobitsyn A, Migliori GB, Raviglione MC, Weyer K. The World Health Organization standards for tuberculosis care and management. Eur Respir J, **2018**; 51. pii: 1800098.

22 Heysell SK, Thomas TA, Sifri CD, Rehm PK, Houpt ER. 18-Fluorodeoxyglucose positron emission tomography for tuberculosis diagnosis and management: a case series. BMC Pulm Med, **2013**; 13: 14.

23 Ganchua SKC, Cadena AM, Maiello P, et al. Lymph nodes are sites of prolonged bacterial persistence during Mycobacterium tuberculosis infection in macaques. PLoS Pathog, **2018**; 14: e1007337.

24 Jain AK, Sreenivasan R, Saini NS, Kumar S, Jain S, Dhammi IK. Magnetic resonance evaluation of tubercular lesion in spine. Int Orthop, **2012**; 36: 261–269.

25 Lin PL, Ford CB, Coleman MT, et al. Sterilization of granulomas is common in both active and latent tuberculosis despite extensive within-host variability in bacterial killing. Nat Med, **2014**; 20: 75–79.

26 Malherbe ST, Shenai S, Ronacher K, et al. Persisting positron emission tomography lesion activity and Mycobacterium tuberculosis mRNA after tuberculosis cure. Nat Med, **2016**; 22: 1094–1100.

27 Sathekge M, Maes A, Kgomo M, Stoltz A, Van de Wiele C. Use of 18F-FDG PET to predict response to first-line tuberculostatic in HIV-associated tuberculosis. J Nucl Med, **2011**; 52: 880–885.

28 Chen RY, Via LE, Dodd LE, et al. Using biomarkers to predict TB treatment duration (Predict TB): a prospective, randomized, noninferiority, treatment shortening clinical trial. Gates Open Res, **2017**; 1: 9.

29 Tucker EW, Guglieri-Lopez B, Ordonez AA, et al. Non-invasive 11C-rifampin positron emission tomography reveals drug biodistribution in tuberculous meningitis. Sci Transl Med, **2018**; 10. pii: eaau0965.

30 Niyonkuru A, Bakari KH, Lan X. 18F-fluoro-2-deoxy-d-glucose pet/computed tomography evaluation of lung cancer in populations with high prevalence of tuberculosis and other granulomatous disease. PET Clin, **2018**; 13: 19–31.

## LEGENDS TO FIGURES

**Figure 1: Serial $^{18}$F-FDG PET/CT scans showing progressive decrease in activity with resolution at end of treatment.** Whole-body projections are shown. **Panel A**: Pre-treatment scan. The yellow arrows indicate, from top to bottom, $^{18}$F-FDG uptake in the left cervical nodes, bilateral hilar nodes and subcarinal nodes. Red arrows indicate left adrenal involvement and an enlarged portal node with corresponding transaxial sections. **Panel B**: Repeat scan after 2 months of therapy with ATT, showing only physiological cardiac activity (a variant) and no residual disease. **Panel C**: Repeat scan at the end of treatment showing no residual FDG-avid disease.

**Figure 2: Serial $^{18}$F-FDG PET/CT scans showing complete resolution of FDG activity at end of 24 months treatment.** Whole-body projections of $^{18}$F-FDG PET/CT scans are shown with corresponding transaxial fused slices (PET and CT) at areas of interest. **A** Baseline FDG PET revealing intense FDG avidity in the L1–L2 vertebrae (blue arrow), with bilateral psoas abscess (red arrows) and few mediastinal and cervical lymph nodes (small black arrows). **B** FDG PET 3 months after starting anti-tubercular treatment showspartial resolution of the above lesions, with avidity at L1–L2 vertebrae and paravertebral soft tissue. Eight months after starting anti-tubercular medication, there was stable disease and the patient remained symptomatic. **C** After 2 years (dose of INH was increased) of ATT, complete metabolic response is noted

**Figure 3: Serial scans in a patient with EPTB involvement of bone (L1–L2). $^{18}$F-FDG PET/CT scan shows complete resolution of FDG activity at end of 24 months of treatment but with residual gibbus deformity.** Whole-body projections of $^{18}$F-FDG PET/CT scans are shown with corresponding sagittal fused slices (PET and CT) at areas of interest. **A** Baseline FDG PET revealing intense $^{18}$F-FDG activity in the L1–L2 vertebrae (blue arrow), with multiple cervical, mediastinal and retroperitoneal lymph nodes (small black arrows). **B** $^{18}$F-FDG PET 2 months after starting anti-TB treatment shows partial resolution of the above-mentioned lesions, with residual $^{18}$F-FDG activity at the L1–L2 vertebrae and mediastinal lymph nodes. **C** Two years after starting anti-tubercular medication there is complete metabolic resolution of the disease, but with gibbus deformity at L1–L2 (dotted blue arrow).

**Figure 4: Serial $^{18}$F-FDG PET/CT scans showing residual activity at end of treatment.** Whole-body projections are shown. **Panel A:** Pre-treatment scan. The yellow arrows indicate, from top to bottom, $^{18}$F-FDG uptake in the bilateral cervical nodes, axillary nodes, subcarinal nodes and retroperitoneal nodes. Small white arrows indicate pulmonary TB. **Panel B**: Repeat scan after 2

months of therapy with ATT. **Panel C**: Repeat scan at the end of treatment (26 weeks), showing residual $^{18}$F-FDG activity in left axillary nodes and retroperitoneal nodes.

**Figure 5: Serial scans in a patient with tuberculoma in the right temporoparietal region.** $^{18}$F-FDG PET/CT scan shows no significant change in FDG activity at end of treatment (the patient subsequently died). Views of the brain with $^{18}$F-FDG PET scans are shown. **A** Transaxial slices; (red) crossed lines indicate site of tuberculoma. **B** The repeat scan after 8 months of therapy with ATT shows no significant change in activity.

**Figure 6: Serial $^{18}$F-FDG PET/CT scans in a patient with mediastinal node EPTB showing no response to treatment. Patient developed MDR-TB. Panels a, b, c:** $^{18}$F-FDG PET/CT scans show uptake in enlarged cervical, supraclavicular and mediastinal nodes (red arrows) with uptake in fibrotic changes in the left lung (small red arrows). **Panels d, e, f**: $^{18}$F-FDG PET/CT scan done 2 months post ATT therapy shows increase in number and size of lymph nodes and appearance of new lung nodules bilaterally. **Panels g, h, i:** $^{18}$F-FDG PET/CT scan done at end of treatment at 7 months shows no significant change in FDG activity in nodes and left lung and new lung nodules (small red arrows). Patient was reassessed for non-compliance with ATT and found to have MDR-TB.

**Figure 7: $^{18}$F-FDG PET/CT scan – transient increase in activity due to superadded chest infection.** Serial scans in a patient on treatment with ATT for EPTB. A transient increase in FDG activity is seen on the 2-month scan due to superadded infection. Whole-body projections (oblique) are shown. **Panel A**: Pre-treatment scan. The yellow arrows indicate $^{18}$F-FDG uptake in the left lung pleura and the red arrow indicates physiological cardiac activity.

**Panel B**: Repeat scan after 2 months of therapy with ATT, showing increased FDG uptake (compared with baseline) in the lower part of the pleura (dashed yellow arrow).

**Panel C**: Repeat scan at the end of treatment, showing residual FDG activity in the left lung pleura (yellow arrows), with a reduction in the extent of avid disease.

**Figure 1: Serial $^{18}$F-FDG PET/CT scans showing progressive decrease in activity with resolution at end of treatment. Whole-body projections are shown.**

**Panel A: Pre-treatment scan. The yellow arrows indicate, from top to bottom, $^{18}$F-FDG uptake in the left cervical nodes, bilateral hilar nodes and subcarinal nodes. Red arrows indicate left adrenal involvement and an enlarged portal node with corresponding transaxial sections.**

**Panel B: Repeat scan after 2 months of therapy with ATT, showing only physiological cardiac activity (a variant) and no residual disease.**

**Panel C: Repeat scan at the end of treatment showing no residual $^{18}$F-FDG-avid disease.**

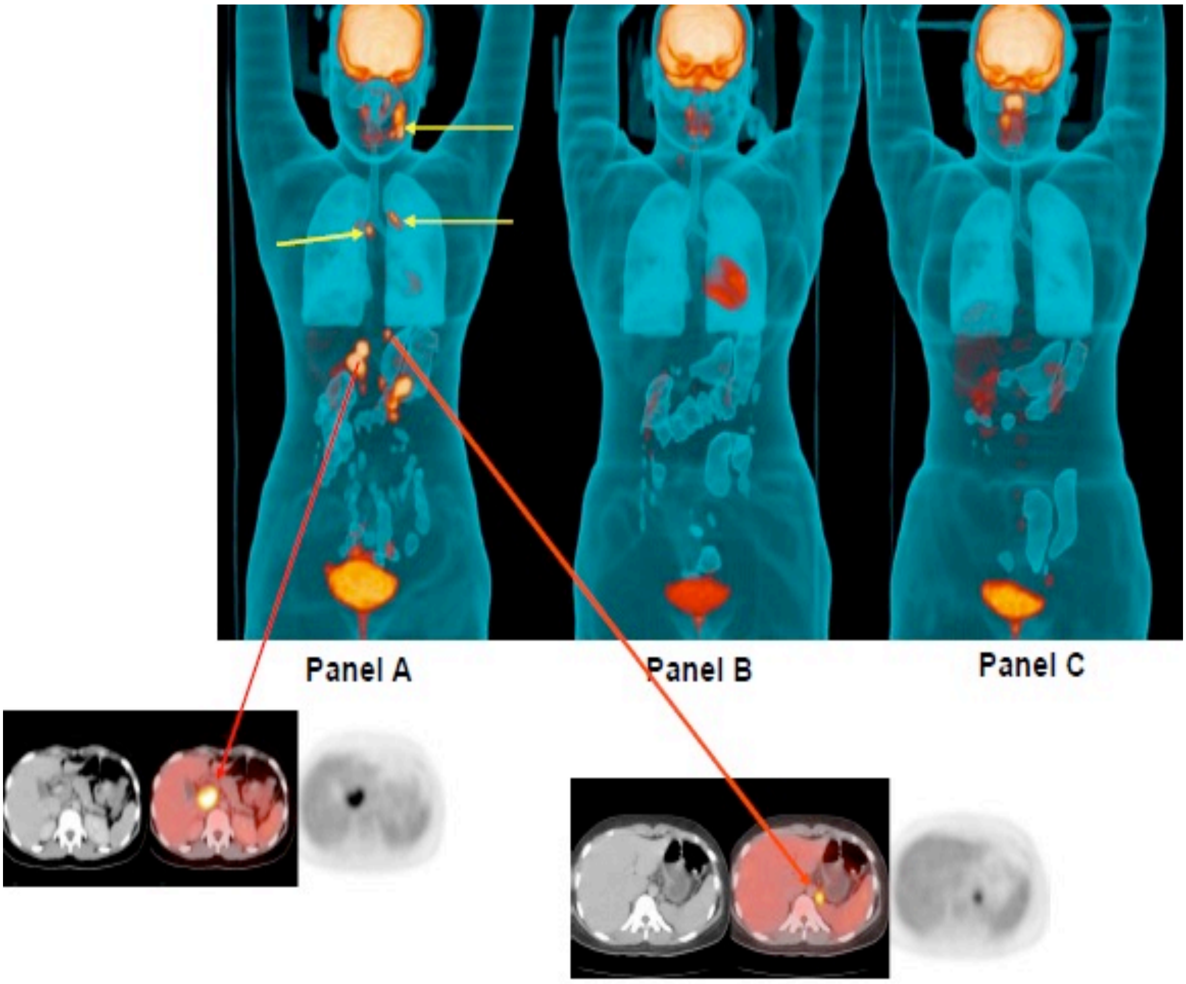

**Figure 2:** **Serial $^{18}$F-FDG PET/CT scans showing complete resolution of $^{18}$F-FDG activity at end of 24 months treatment.**

**Whole-body projections of $^{18}$F-FDG PET/CT scans are shown with corresponding transaxial fused slices (PET and CT) at areas of interest. A Baseline $^{18}$F-FDG PET revealing intense $^{18}$F-FDG avidity in the L1–L2 vertebrae (blue arrow), with bilateral psoas abscess (red arrows) and few mediastinal and cervical lymph nodes (small black arrows). B $^{18}$F-FDG PET 3 months after starting anti-tubercular treatment shows partial resolution of the above lesions, with avidity at L1–L2 vertebrae and paravertebral soft tissue. Eight months after starting anti-tubercular medication, there was stable disease and the patient remained symptomatic. C After 2 years (dose of INH was increased) of ATT, complete metabolic response is noted**

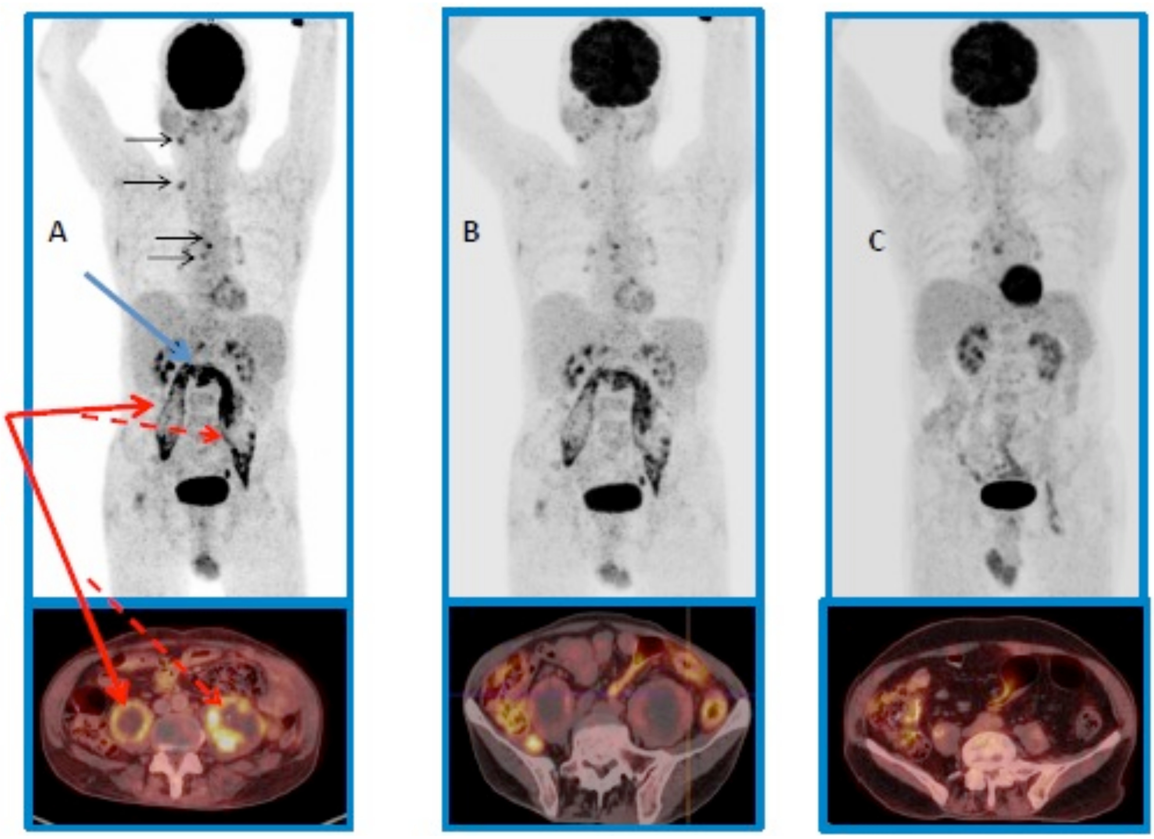

**Figure 3: Serial scans in a patient with EPTB involvement of bone (L1–L2). $^{18}$F-FDG PET/CT scan shows complete resolution of FDG activity at end of 24 months of treatment but with residual gibbus deformity.**

Whole-body projections of $^{18}$F-FDG PET/CT scans are shown with corresponding sagittal fused slices (PET and CT) at areas of interest. **A** Baseline FDG PET revealing intense $^{18}$F-FDG activity in the L1–L2 vertebrae (blue arrow), with multiple cervical, mediastinal and retroperitoneal lymph nodes (small black arrows). **B** $^{18}$F-FDG PET/CT, 2 months after starting anti-TB treatment shows partial resolution of the above-mentioned lesions, with residual $^{18}$F-FDG activity at the L1–L2 vertebrae and mediastinal lymph nodes. **C** Two years after starting anti-tubercular medication there is complete metabolic resolution of the disease, but with gibbus deformity at L1–L2 (dotted blue arrow).

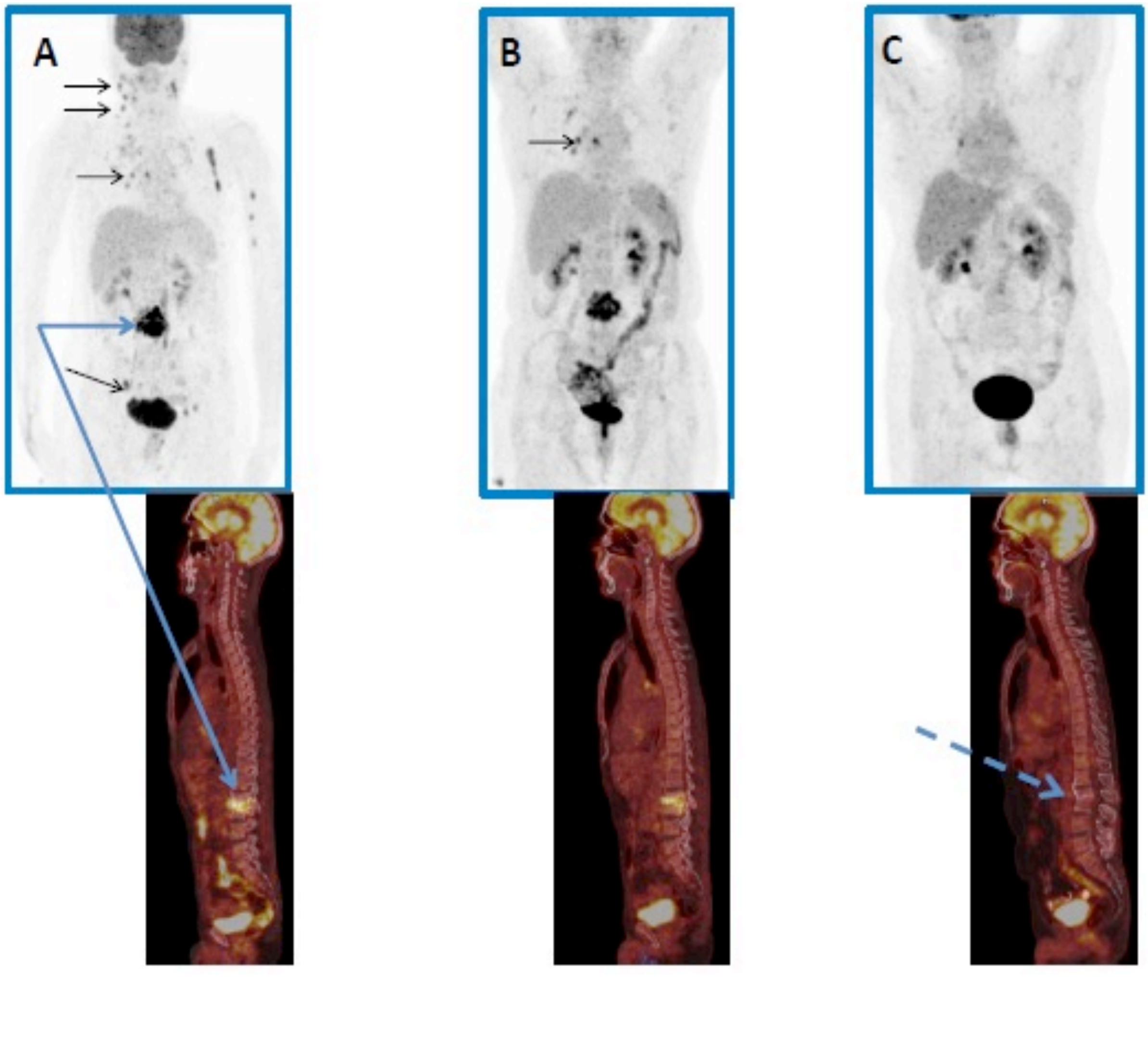

**Figure 4: Serial $^{18}$F-FDG PET/CT scans showing residual activity at end of treatment.**

Whole-body projections are shown. **Panel A:** Pre-treatment scan. The yellow arrows indicate, from top to bottom, $^{18}$F-FDG uptake in the bilateral cervical nodes, axillary nodes, subcarinal nodes and retroperitoneal nodes. Small white arrows indicate pulmonary TB. **Panel B**: Repeat scan after 2 months of therapy with ATT. **Panel C**: Repeat scan at the end of treatment (26 weeks), showing residual FDG activity in left axillary nodes and retroperitoneal nodes.

Figure 3

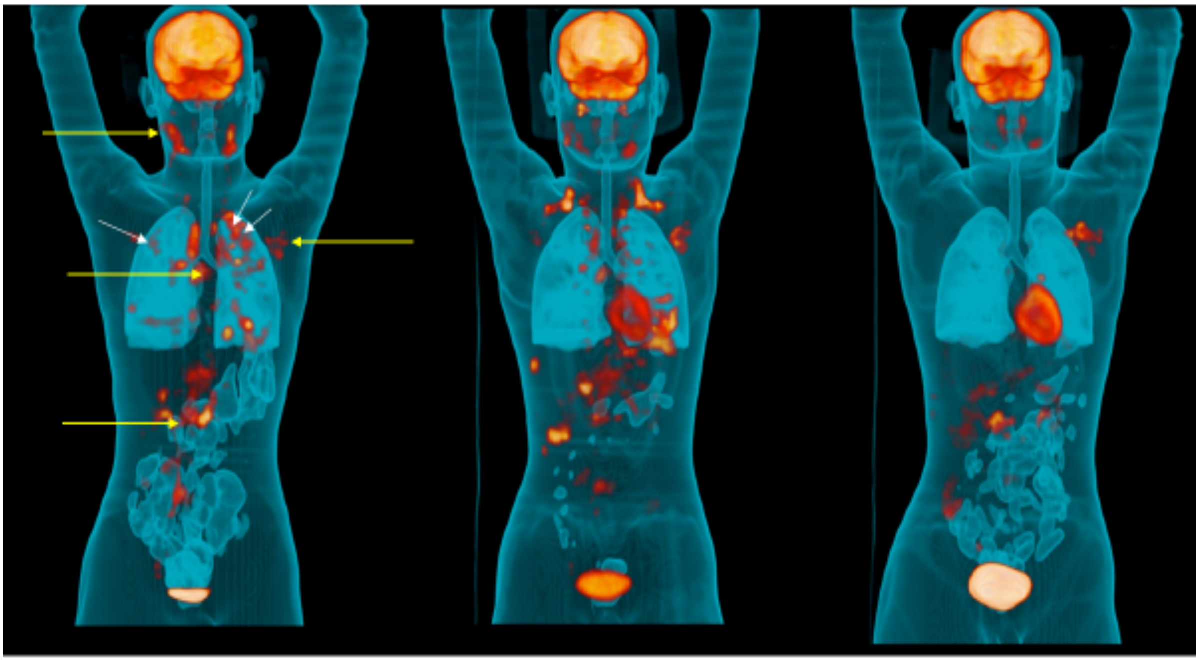

Panel A Panel B Panel C

**Figure 5: Serial scans in a patient with tuberculoma in the right temporoparietal region.**

$^{18}$F-FDG PET/CT scan shows no significant change in FDG activity at end of treatment (the patient subsequently died). Views of the brain with $^{18}$F-FDG PET/CT scans are shown. **A** Transaxial slices; (red) crossed lines indicate site of tuberculoma. **B** The repeat scan after 8 months of therapy with ATT shows no significant change in activity.

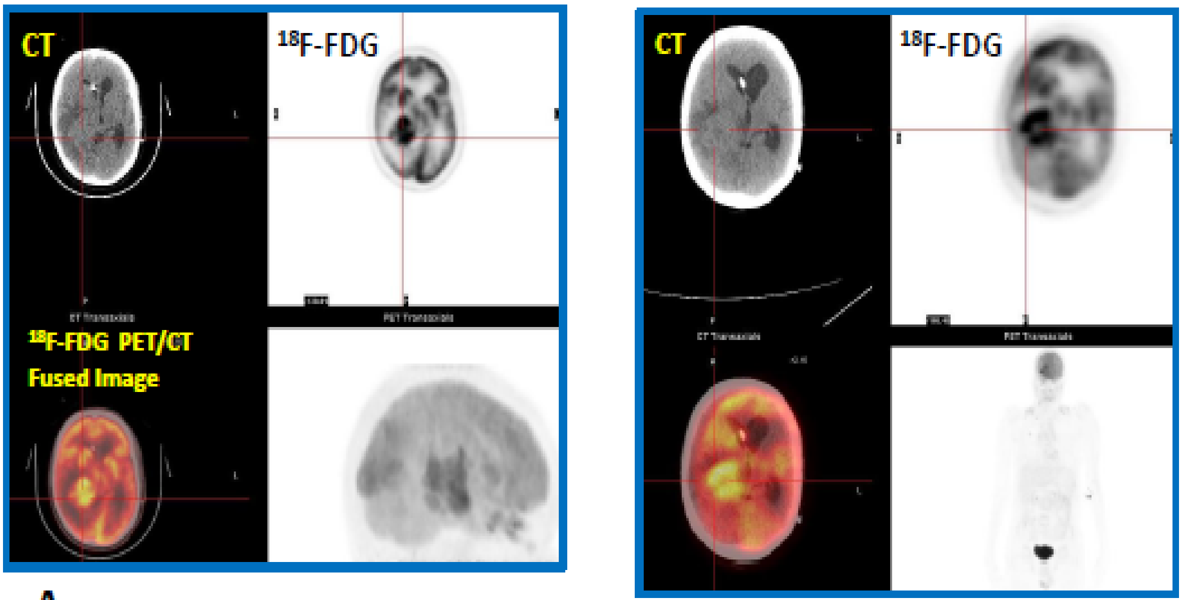


A 30/3/2016
BASELINE

B 01/12/2016
POST TREATMENT

**Figure 6**

**MDR-TB 2: Serial $^{18}$F-FDG PET/CT scans in a patient with mediastinal node EPTB showing no response to treatment. Patient developed MDR-TB.**

**Panels A, B, C:** $^{18}$F-FDG PET/CT scans show uptake in enlarged cervical, supraclavicular and mediastinal nodes (red arrows) with uptake in fibrotic changes in the left lung (small red arrows).

**Panels D, E, F**: $^{18}$F-FDG PET/CT scan done 2 months post ATT therapy shows increase in number and size of lymph nodes and appearance of new lung nodules bilaterally.

**Panels G, H, I:** $^{18}$F-FDG PET/CT scan done at end of treatment at 7 months shows no significant change in FDG activity in nodes and left lung and new lung nodules (small red arrows). Patient was reassessed for non-compliance with ATT and found to have MDR-TB.

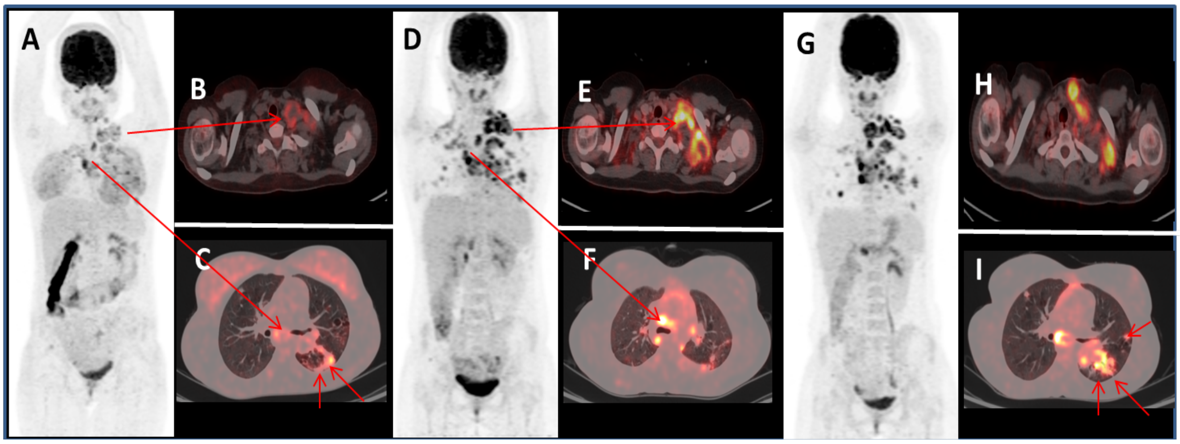

**Figure 7: $^{18}$F-FDG PET/CT scan – transient increase in activity due to superadded chest infection.**

Serial scans in a patient on treatment with ATT for EPTB. A transient increase in $^{18}$F-FDG activity is seen on the 2-month scan due to superadded infection. Whole-body projections (oblique) are shown.
**Panel A**: Pre-treatment scan. The yellow arrows indicate $^{18}$F-FDG uptake in the left lung pleura and the red arrow indicates physiological cardiac activity.
**Panel B**: Repeat scan after 2 months of therapy with ATT, showing increased $^{18}$F-FDG uptake (compared with baseline) in the lower part of the pleura (dashed yellow arrow).
**Panel C**: Repeat scan at the end of treatment, showing residual FDG activity in the left lung pleura (yellow arrows), with a reduction in the extent of avid disease.

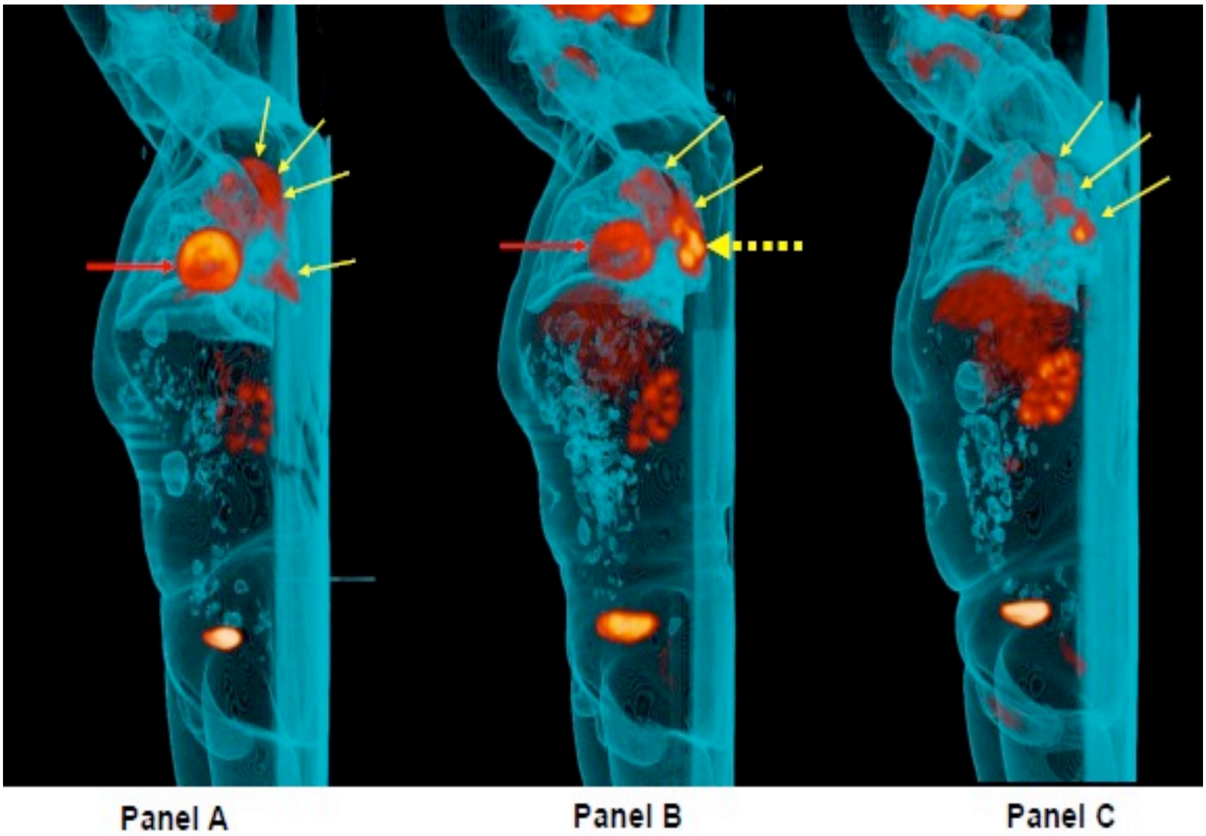

**Table 1: Clinical algorithm for imaging pathway:**

1. Patient presenting/referred to Respiratory/TB clinic with chronic cough of more than 2 weeks, weight loss, night sweats, fever, SOB, headache, altered mental state, pain in bone/joint and a lump or mass. History of close TB contact, clinicians' clinical suspicion of EPTB for any other reason.
2. Symptomatology assessed by local chest physicians.
3. Clinical assessment, chest radiography, tuberculin skin test, HIV test, cultures, GeneXpert MTB Rif/assay and other investigations as clinically indicated to confirm presence of *Mycobacterium tuberculosis* (sputum, histopathology, cytology, FNAC and histopathology for skin, genitourinary and breast tuberculosis, X-ray for bone tuberculosis, synovial biopsy for joint tuberculosis, cerebrospinal fluid cytology and biochemistry for tuberculous meningitis, with or without contrast-enhanced computed tomography (CT) findings, spinal features (gibbus) with or without radiological findings, magnetic resonance imaging (MRI) of brain and MRI of spine. Pleural and ascitic fluid for tuberculous pleural effusions and abdominal tuberculosis.
4. Except for suspect meningitis, no treatment initiated before $^{18}$F-FDG PET/CT scan.
5. Consent obtained, patient informed of repeat scan at 2 months and end of treatment.
6. Patients with high likelihood of EPTB on clinical grounds and confirmed -ve HIV status, referred to Nuclear Medicine Imaging Department for $^{18}$F-FDG PET/CT scan

↓

7. **Scan 1: First $^{18}$F-FDG PET/CT scan** performed as soon as possible after referral (immediately for TB meningitis suspects or those critically ill)
6. Scans reported locally and sent to referrer/TB clinic within 24 h
7. Results of other investigations available
8. CRF completed after results.
9. TB treatment initiated (visit 1) or stopped if treatment completed (visit 3)
10. **Follow-up PET Scans:**
**Scan 2**: at 2 months after start of TB treatment
**Scan 3**: at end of TB treatment

**Table 2:**
**Time to scan and number of active sites in 147 patients with EPTB who underwent three $^{18}$F-FDG PET/CT scans during course of treatment**

| | **Baseline $^{18}$F-FDG PET/CT scan** | **2$^{nd}$ visit $^{18}$F-FDG PET/CT scan** | **End of treatment $^{18}$F-FDG PET/CT scan** |
|---|---|---|---|
| **Time to scan** | 1–15 days post referral | Median time to scan = 2. 4 months | Median time to scan = 7.4 months |
| **$^{18}$F-FDG PET/CT scan** | Total Scans =147 | Scan +ve = 120/147 | Scan +ve =94/147 |
| **Total number of active sites** | 1 site =44<br>2 sites =33<br>3 sites =20<br>4 sites =20<br>>4 sites =24 | 1 site =53<br>2 sites =24<br>3 sites =19<br>4 sites =8<br>>4 sites =16 | 1 site =46<br>2 sites =27<br>3 sites =9<br>4 sites =8<br>>4 sites =4 |
| **$^{18}$F-FDG activity ($SUV_{max}$)***<br>**Range ($SUV_{max}$)**<br>**Median ($SUV_{max}$)**<br>**Mean ($SUV_{max}$)** | 2·6–32.0<br>9·9<br>9.9 | 2·5–25.0<br>6·2<br>7·1 | 2·5–17<br>5·0<br>6·2 |
| **Sum of $SUV_{max}$****<br>**(% fall/decrease)** | 19·4 | 15·8<br>(18·6%) | 8·8<br>(54·6%) |

$^{18}$F-FDG PET/CT scan:
Scan +ve pattern: Refers to scans which showed at least one lesion with increased $^{18}$F-FDG activity or ongoing activity ($SUV_{max} \geq 2.5$)
* $SUV_{max}$ distribution is given for the maximum of the $SUV_{max}$ values across the sites
** The sum of $SUV_{max}$ values is predicted from the multilevel mixed effects linear regression model, fitted to all patients who had at least two PET scans

Table 3:

**Baseline $^{18}$F-FDG PET scan and anatomical location of active sites in 147 patients with EPTB**

| Anatomical site | PET/CT positive | | $SUV_{max}$ | | |
|---|---|---|---|---|---|
| | Number of patients | % of patients | Range | Mean | Median |
| **Brain** | 7 | 4.8 | 4-15.2 | 10.6 | 11.4 |
| **Pleura** | 16 | 10.9 | 3.1-17.7 | 7.0 | 6.7 |
| **Muscles*** | 5 | 3.4 | 3.4-11.2 | 7.0 | 6.9 |
| **Liver** | 2 | 1.4 | 3.8-13.1 | 8.4 | 8.4 |
| **Spleen** | 3 | 2.0 | 2.7-5.6 | 4.1 | 4 |
| **Gastrointestinal tract** | 5 | 3.4 | 3.4-17.4 | 11.7 | 12.6 |
| **Urogenital tract** | 4 | 2.7 | 7.1-10.5 | 8.8 | 8.9 |
| **Bone** | 51 | 34.7 | 2.5-22.5 | 8.7 | 8.6 |
| **Lymph nodes** | 99 | 67.3 | 2.8-22.3 | 9.1 | 7.7 |
| Cervical | 57 | 38.8 | 2.6-22.3 | 8.4 | 7.6 |
| Supraclavicular | 32 | 21.8 | 3.1-19.3 | 8.1 | 5.8 |
| Axillary | 26 | 17.7 | 2.5-16 | 7.2 | 5.6 |
| Mediastinal | 68 | 46.3 | 2.5-21.2 | 6.9 | 6.3 |
| Hilar | 27 | 18.4 | 2.7-17.8 | 6.3 | 5.4 |
| Retrocrural | 5 | 3.4 | 3.1-15.7 | 6.7 | 4.3 |
| Retroperitoneal/mesenteric | 31 | 21.1 | 3-15.5 | 6.8 | 5.9 |
| Pelvic | 16 | 10.9 | 2.5-21.5 | 6.6 | 5.2 |
| Inguino-femoral | 7 | 4.8 | 2.6-7.6 | 4.9 | 4.9 |
| **Other sites**** | 6 | 4.1 | 2.5-32 | 10.2 | 5.3 |

**Table 4:**

**Second $^{18}$F-FDG PET scan and anatomical location of active sites in 147 patients with EPTB**

| Anatomical site | PET/CT positive | | $SUV_{max}$ | | |
|---|---|---|---|---|---|
| | No of patients | % of patients | Range | Mean | Median |
| **Brain** | 6 | 4.1 | 4.2-12 | 9.9 | 10.6 |
| **Pleura** | 18 | 12.2 | 2.8-12.5 | 6.4 | 5.9 |
| **Liver** | 2 | 1.4 | 6.7-10.4 | 8.6 | 8.6 |
| **Spleen** | 0 | 0 | - | - | - |
| **Gastrointestinal tract** | 4 | 2.7 | 5.7-10.2 | 7.8 | 7.8 |
| **Urogenital tract** | 4 | 2.7 | 2.9-5.9 | 4.9 | 5.4 |
| **Bone** | 39 | 26.5 | 2.6-15.5 | 6.5 | 5.6 |
| **Lymph nodes** | 82 | 55.8 | 2.5-25 | 6.5 | 5.2 |
| Cervical | 37 | 25.2 | 2.6- 14.6 | 5.4 | 4.4 |
| Supraclavicular | 22 | 15.0 | 2.5-13.7 | 6.1 | 5.7 |
| Axillary | 16 | 10.9 | 3.1-13.2 | 5.5 | 4 |
| Mediastinal | 46 | 31.3 | 2.5-25 | 6.6 | 5.2 |
| Hilar | 21 | 14.3 | 2.5-14.1 | 5.6 | 4.6 |
| Retrocrural | 4 | 2.7 | 2.9-10.1 | 4.8 | 3.2 |
| Retroperitoneal/mesenteric | 23 | 15.6 | 3-15.5 | 6.1 | 5.7 |
| Pelvic | 9 | 6.1 | 2.8-11.2 | 4.5 | 3.4 |
| Inguino-femoral | 8 | 5.4 | 2.5-7.9 | 3.7 | 3.3 |
| | | | | | |

**Table 5.**

**Third $^{18}$F-FDG PET scan and anatomical location of active sites in 147 patients with EPTB at end of treatment**

| Anatomical site | PET/CT positive | | $SUV_{max}$ | | |
|---|---|---|---|---|---|
| | No. of patients | % of patients | Range | Mean | Median |
| **Brain** | 5 | 3.4 | 3.2-15 | 8.5 | 9.9 |
| **Pleura** | 10 | 6.8 | 3.7-11.4 | 5.7 | 5.2 |
| **Liver** | 0 | 0 | - | - | - |
| **Spleen** | 0 | 0 | - | - | - |
| **Gastrointestinal tract** | 3 | 2.0 | 3.1-10 | 6.8 | 10.4 |
| **Urogenital tract** | 2 | 1.4 | 2.7-4 | 3.4 | 3.4 |
| **Bone** | 28 | 19.0 | 2.5-9.5 | 5.4 | 4.9 |
| **Lymph nodes** | 67 | 45.6 | 2.5-16.5 | 5.9 | 4.9 |
| Cervical | 29 | 19.7 | 2.5-13.5 | 4.1 | 3.4 |
| Supraclavicular | 10 | 6.8 | 2.8-10.7 | 6.0 | 5.4 |
| Axillary | 10 | 6.8 | 2.7-6.8 | 4.6 | 4.4 |
| Mediastinal | 37 | 25.2 | 2.8-16.5 | 6.3 | 4.7 |
| Hilar | 16 | 10.9 | 3.2-8.6 | 5.6 | 5.4 |
| Retrocrural | 0 | 0 | - | - | - |
| Retroperitoneal/mesenteric | 11 | 7.5 | 2.5-13.6 | 5.9 | 3.9 |
| Pelvic | 4 | 2.7 | 2.5-4.7 | 3.5 | 3.4 |
| Inguino-femoral | 2 | 1.4 | 3.3-5 | 4.2 | 4.2 |

**SUPPLEMENTAL APPENDIX**

**Supplemental Figure 1:**

**Changes in the sum of PET/CT $SUV_{max}$ values over time obtained from three scans for all 147 patients. The vertical lines, with arrows, point to the overall predicted sum of $SUV_{max}$ at the median times of the second and third visits (2.5 months and 7.4 months, respectively). For the visual presentation the individual patients' data are restricted to those where the sum of $SUV_{max}$ is less than 50; the linear prediction for centres and the overall linear prediction were estimated with all data included. Progressive reduction in activity was seen in the majority of patients after 2 months of treatment. The reduction in the sum of $SUV_{max}$ was on average 1.4/month (slope = -1.4, 95% CI -1.8/month -1.1/month) with variance of the random slope at the centre level of 0.11 (95% CI 0.02–0.63; LR test for random slope: $\chi^2$=4.42, p=0.036).**